ELSEVIER

Contents lists available at ScienceDirect

# Sensors and Actuators B: Chemical

journal homepage: www.elsevier.com/locate/snb



# Electrochemical cotinine sensing with a molecularly imprinted polymer on a graphene-platinum nanoparticle modified carbon electrode towards cigarette smoke exposure monitoring



Kshama Parate<sup>a</sup>, Chandran Karunakaran<sup>b</sup>, Jonathan C. Claussen<sup>a,\*</sup>

- <sup>a</sup> Department of Mechanical Engineering, Iowa State University, Ames, IA, 50011, USA
- <sup>b</sup> Biomedical Research Laboratory, Department of Chemistry, VHNSN College (Autonomous), Virudhunagar, 626 001, Tamil Nadu, India

#### ARTICLE INFO

# Keywords: Graphene Platinum nanoparticles Molecular imprinted polymer Cotinine Electrochemical biosensor

#### ABSTRACT

Cotinine, a metabolite of nicotine, has shown promise as a biomarker for the detection of tobacco use and smoke exposure due its ability to persist in human bodily fluids for days ( $\it ca.$  4–5 days) after tobacco consumption. However, current cotinine detection strategies primarily include arduous laboratory sensing methods or qualitative in-field biosensing devices. Herein, we report an electrochemical cotinine sensor based on a selective molecularly-imprinted polymer (MIP) electrodeposited on a screen-printed carbon electrode (SPCE) modified with graphene flakes and platinum nanoparticles (PtNPs). The PtNP-graphene modified SPCE exhibited a 4-fold increase in electrochemical sensitivity ( $10\,\mu\text{A}-40\,\mu\text{A}$ ) during ferricyanide cyclic voltammetry. This developed biosensor functionalized with the MIP was consequently capable of selective sensing of cotinine in spiked saliva samples across a wide sensing range ( $1-100\,n\text{M}$ ) and low detection limit of ( $0.33\,n\text{M}$ ). This sensing range covers cotinine concentration levels that are typically found in saliva for non-smokers and smokers ( $\it ca.$  10–75 nM). Moreover, the sensing is capable of acquiring a cotinine measurement within 12 min with minimal interference from both nicotine and myosmine— cotinine chemical analogs that are typically found in tobacco products. Hence, the developed biosensor is well-suited for use in the field such as at point-of-care facilities.

# 1. Introduction

The consumption of tobacco products and exposure to tobacco smoke has been linked to a wide variety of diseases including numerous cancers (lung, liver, pancreatic) and cardiovascular disease [1–5]. Governments around the globe have taken measures to restrict the exposure of cigarette smoke by banning its use in myriad public localities. Moreover, health care providers and insurance providers alike are searching for methods to not only verify those who use tobacco products but also to quantify exposure to environmental or second-hand tobacco smoke. The ability to quantify the use of tobacco could help healthcare providers more accurately identify smoking alternatives (e.g., nicotine patches) and quantify the nicotine dosage (the addictive drug found in tobacco products) needed in said alternatives to help patients overcome their tobacco smoking habits. Moreover, a quantifiable smoking test could help insurance providers accurately set premiums based upon smoking status [6,7].

Cotinine, a byproduct of nicotine metabolism, has shown tremendous promise as a biomarker for monitoring the consumption of tobacco products as it has a much longer physiological half-life (24 h) than nicotine (2h). Consequently cotinine has been detected in a variety of human bodily fluids (e.g., blood, urine and saliva) 4-5 days after direct tobacco consumption, smoke inhalation, or indirect smoke exposure [8,9]. Recent research has indicated that cotinine is a reliable indicator of smoke exposure [10-14] and that median concentrations of cotinine in human saliva are approximately 13.6 nM in non-smokers,  $20.4\,\mathrm{nM}$  in those affected by secondhand smoke, and  $40\text{--}74\,\mathrm{nM}$  in smokers depending upon various factors such as gender, age, and smoke exposure duration/intensity (e.g., number of cigarettes smoked) [15]. Such cotinine concentration measurements are typically obtained from laboratory techniques such as liquid/gas chromatography, piezoelectric microgravimetry, surface plasmon resonance (SPR), or chemiluminescence immunoassays [16-22]. These laboratory techniques are generally time consuming and expensive as they require extensive sample preparation and cleanup as well as specialized personnel and instrumentation. Moreover, some of these assays use biological components such as antibodies that limit the shelf-life of the sensor or require the use of pre-labeling where cotinine needs to be pre-conjugated

E-mail address: jcclauss@iastate.edu (J.C. Claussen).

<sup>\*</sup> Corresponding author.

with fluorescent probes such as quantum dots in order to enable a sensor measurement [23]. Hence these cotinine sensing techniques are not amenable to wide-scale, low-cost screening of cotinine in smokers.

Recent progress has been made for the development of in-field, nonlaboratory based sensing of cotinine. Some of these techniques have been commercialized including colorimetric biosensors such as the Saliva SmokeScreen, the NicAlert Saliva Test Strip, and a cotinine sensor from Alere Toxicology. The Saliva SmokeScreen biosensor yields a colorimetric result garnered from a saliva swab sample that can semiquantify the cotinine levels of a patient into general categories (i.e., heavy smoking, moderate smoking, and light smoking) [24]. The NicAlert Saliva Test Strip similarly uses a "dipstick" colorimetric immunoassay reaction to determine a relative range of possible cotinine concentrations present in saliva [25,26] while the cotinine sensor from Alere Toxicology, also provides a qualitative cotinine response via enzyme immunoassay detection [27]. However, recent research with molecularly imprinted polymers (MIPs) has shown promise for the development of a fully quantifiable in-field cotinine sensor. Such a truly quantifiable cotinine biosensor would be crucial to pinpointing the level of smoke exposure experienced by a patient.

MIP-based electrochemical biosensors have become increasingly important to the greater biosensor field [28]. An MIP is a synthetic polymer consisting of a template molecule embedded in a polymer. The template molecule is extracted from the polymer matrix leaving behind template-shaped cavities and functional group attachment sites that are specific to target analytes of interest. MIP-based biosensors in general display high stability and shelf-life as they are comprised of synthetic polymers (e.g., methacrylic acid, poly – 4-vinylphenol, polypyrrole) that are much more resilient to fluctuations in temperature and pressure than conventional biological-based biorecognition agents such as antibodies and enzymes [16,18-20,29,30]. Consequently, MIP-based cotinine biosensors have been developed, however, such biosensors have only exhibited the ability to selectively monitor cotinine at high concentrations (tending towards heavy smokers) [17,31]. Hence these MIPbased biosensors would be unable to monitor lower cotinine concentrations such as those exposed to secondhand smoke. These biosensors also utilize optical and microgravimetry sensing modalities that require laboratory equipment and hence are not conducive to in-field biosensing. Other drawbacks to MIP-based biosensors in general include MIP synthesis protocols that often entail polymer preparation processes such as thermal polymerization, sedimentation, "natural" polymerization, and precipitation polymerization which are time consuming or complex (requiring multiple process steps) and that potentially limit sensitivity of the resultant biosensor [5,19,32-36]. For example, these multi-step MIP synthesis processes can result in an uneven or a highly thick MIP layer (> 60 μm) deposited on the biosensor surface that consequently can impede the reaction-diffusion kinetics of incident target analyte and ultimately dampen the biosensor sensitivity [37,38]. Furthermore, depending on the sensing modality, a separate instrument may be required for measuring signals from the MIP such as a high-performance liquid chromatography (HPLC) system, where the analyte is passed through a chromatography column to separate the analyte and then analyzed with a Raman spectrometer [33]. Such biosensing techniques require trained technicians working in a laboratory environment and hence are not conducive to rapid, in-field biosensing needed for point-of-service sensing paradigms. On the other hand, electrochemically deposited MIPs have been shown to at least partially circumvent these issues by providing a method to deposit a MIP layer in a controlled, consistent, and facile manner that consequently limits slow biosensor diffusion kinetics [18,39]. Moreover, these MIPs are also generally utilized to monitor target analyte within an electrochemical sensing modality which yields a digital concentration readout from a portable handheld potentiostat, like a home glucose monitor, to rapidly quantify cotinine concentrations in the field.

Herein, we report the creation of a MIP-based biosensor that is capable of rapid and quantifiable detection of cotinine concentrations in saliva samples. The biosensor is fabricated with a facile, one-step electrochemical MIP manufacturing protocol that uses a PtNP-graphene nanohybrid material as the transduction element. A solution-phase graphene ink is drop coated, laser annealed, and electrochemically decorated with PtNPs on a screen-printed carbon electrode (SPCE) to increase the surface area and electroreactivity of the electrode. We have shown that such laser processing of printed graphene significantly increases the defects and superficial oxygen species of the electrode [40,41] as well as changes the surface wettability from hydrophilic [static contact angle (CA) ~ 45°] to one that is hydrophobic [CA > 90°], a material property that can improve the biosensor selectivity [42]. Such a graphene surface peppered with oxygenated species and defects is well-suited to act as a carbon scaffold surface for subsequent electrochemical deposition of PtNPs—nanoparticles that are well known for their high catalytic behavior in fuel cells [43,44], chemical propulsion systems [45-47], and biosensors [48-50]. Next, an ortho-phenylenediamine (oPD) MIP is evenly electrodeposited onto the PtNP/graphene-SPCE to complete the cotinine biosensor. This resultant biosensor can detect cotinine down to subnanomolar ranges (~ 0.33 nM) which is lower than any reported cotinine biosensor to date [23]. Moreover, the biosensor displayed high selectivity to cotinine over nicotine and myosmine, which are close chemical analogs to cotinine, as well as high selectivity in actual saliva matrix.

## 2. Experimental methods

#### 2.1. Materials

The following materials were purchased from Sigma Aldrich (USA): o-Phenylenediamine, sodium acetate, potassium chloride, and potassium ferrocyanide. Cotinine was obtained from Alfa Aesar (USA). All solutions were prepared in DI water. Screen printed carbon electrodes (SPCEs) formatted in a 3-electrode arrangement with a carbon working electrode (3 mm in diameter), carbon auxiliary electrode, and a silver/silver chloride (Ag/AgCl) reference electrode all printed on the same surface were obtained from CH Instruments (Austin, TX).

# 2.2. PtNP-graphene SPCE fabrication and MIP biofunctionalization

Graphene ink was created by mixing completely reduced graphene oxide with ethyl cellulose and terpineol according to our previous protocols [40]. A small aliquot (1 µl) of the graphene ink was drop cast onto the SPCE and dried at 80 °C for 30 min. Next, the graphene modified SPCE was laser annealed for 10 ms using a 1000 mW diode laser engraver (HTPOW). A 4 mM chloroplatinic acid and  $0.5\,M$  Na $_2SO_4$  solution was used to electrochemically deposit PtNPs onto the graphene modified SPCEs (working electrodes). PtNPs were deposited onto the working electrodes via a multi-step current pulse for 250 cycles where each pulse had a duration of 0.5 s and a current density of 10 mA/cm<sup>2</sup>. Next, the MIP electropolymerizing solution was prepared by mixing 7.5 µl of 100 mM of oPD in 87.5 µl of sodium acetate buffer (0.5 M, pH 5.2). Cotinine (0.1 mM) was then dissolved in methanol and 5 µl was added to this mixture. A control electrode comprised of a non-imprinted polymer (NIP) was created by the same process as the MIP except cotinine was excluded from the mixture. The cotinine-oPD mixture was electropolymerized onto the PtNP/graphene -SPCE via cyclic voltammetry where the voltage was swept between 0 and 1.1 V vs. Ag/AgCl at a scan rate of 50 mV/s for 20 cycles. Finally, the MIP was completed by extracting the cotinine from the deposited oPD by placing the electrode in a gently stirred ethanol bath for 10 min at 60 rpm. The MIP-modified electrode was then washed in DI water and dried in nitrogen gas before use. Similarly, the NIP electrode followed the same processing steps but without the cotinine extraction process.

#### 2.3. Electrochemical characterization and cotinine sensing

Electrochemical characterization and biosensing with the PtNP/graphene-SPCE were performed using a CHI6273E potentiostat (CH Instruments, Austin, TX). Cyclic voltammograms (CVs) were recorded for electrodes coated with both the MIP and NIP. CV measurements were performed in the presence of  $1\,\mathrm{mM}\,\mathrm{K}_3[\mathrm{Fe}(\mathrm{CN})_6]/\mathrm{K}_4[\mathrm{Fe}(\mathrm{CN})_6]$  (1:1) solution that also contained 0.1 M KCl over the potential range of  $-0.35\,\mathrm{V}$  and 0.6 V vs. Ag/AgCl at a scan rate of 50 mV/s. Cotinine biosensing was conducted with MIP-modified electrodes incubated in different concentrations (0.1 nM, 1 nM, 5 nM, 10 nM, 50 nM, 100 nM, 1  $\mu$ M, 10  $\mu$ M) of cotinine in phosphate buffer solution for 10 min. The variation of peak current was recorded to determine the calibration curve for the cotinine concentration in the solution.

# 2.4. Cotinine sensing in saliva

Normal human saliva of a non-tobacco user was acquired and processed further by centrifuging at 500 rpm for 10 s to sediment any heavy solid particles if any from the saliva sample. Next the supernatant was pipetted out of the centrifuge tube and spiked with various cotinine concentrations (1 nM, 5 nM, 10 nM, 50 nM, 1  $\mu$ M). These spiked samples were consequently incubated on the MIP-modified electrodes for 10 min. During subsequent electrochemical sensing, the variation of the peak current of the CVs were recorded as noted in Section 2.3 to determine the calibration curve for cotinine concentration in saliva.

#### 3. Results and discussion

#### 3.1. Fabrication and biofunctionalization of the PtNP/graphene SPCE

The cotinine biosensor was developed from a SPCE that was functionalized with both graphene and PtNPs to increase the electroactivity and sensitivity of the electrode in subsequent electrochemical cotinine sensing (Fig. 1a–e). First, a graphene ink (graphene concentration: 15 mg/ml), developed according to our previous protocols (see [41,51] and Experimental Methods), was drop cast onto the SPCE. The graphene coated SPCE was next annealed with a benchtop rapid-pulse laser technique similar to our previous techniques [52]. The laser annealing process thermally removes the solvents and non-conductive binders (ethyl cellulose) present in the ink. We have shown such laser processing stitches or welds the graphene flakes together to increase its electrical conductivity from relatively non-conductive (sheet resistance  $\sim 25\,\mathrm{M}\Omega/\mathrm{sq.}$ ) to highly conductive (sheet resistance  $<1\,\mathrm{k}\Omega/\mathrm{sq.}$ )

[41,42]. PtNPs (~ 400 nm in diameter) were subsequently electrodeposited onto the graphene-SPCE to increase the electroactive nature of the electrode (see Fig. 3) [48,53–55].

Next, the MIP was electrotropolymerized onto the PtNP/graphene-SPCE. Fig. 1f shows the CV for electropolymerization of oPD in the presence of cotinine on the PtNP/graphene-SPCE. This CV displays a prominent oxidation peak of 200 µA at 0.2 V during the first cycle, which progressively decreases during subsequent cycles. The general shape of the CV with no visible reduction peak indicates the polymerization process is irreversible (only deposition is occurring). Such a CV peak is typical for oPD polymerization [56,57]. More specifically, as more layers of non-conducting oPD are deposited onto the electrode, the resistance to heterogenous charge transfer from the solution and electrode increases and hence the oxidation peaks in the CV decreases (see red arrow in Fig. 1f). It should be noted that the oPD is mixed with cotinine and then electropolymerized onto the electrode to form the MIP, while oPD without cotinine is electropolymerized onto the electrode to form a control sensor or non-imprinted polymer (NIP) sensor. The CV generated from the NIP electropolymerization process (Fig. S1 in Supplemental information) is similar to the CV generated during the MIP electropolymerization process demonstrating that oPD deposition is occurring for both the MIP and NIP functionalized electrodes.

Extraction of template molecules follows polymerization. An extracting solution is used to dissolve away the cotinine molecules trapped in the MIP and hence to create pockets for a redox probe to reach the surface of the electrode [58,59]. This process is generally a non-linear process due to diffusion limitations caused by slow mass transfer of analytes diffusing through the membrane into the bulk solution [60]. Various solutions were explored for extracting cotinine from the MIP matrix such as toluene, methanol, and NaOH in a mixture of ethanol/water (2:1) [16,39]. These solutions were either ineffective in removing cotinine from the MIP matrix or they degraded the oPD matrix completely. However, a more viable solvent (pure ethanol) for the cotinine template removal was found and used herein.

# 3.2. Optical and electrochemical characterization of the MIP modified PtNP/graphene-SPCE

The SEM images shown in Fig. 2 represent the surface topography of the electrode with bare unmodified SPCEs, after functionalization with graphene and laser annealing processing, and finally after subsequent functionalization with PtNPs (dia. ~ 400 nm). Note that the surface of the unmodified SPCE electrode is very rough and uneven (Fig. 2a). Upon coating the surface with graphene ink and laser annealing

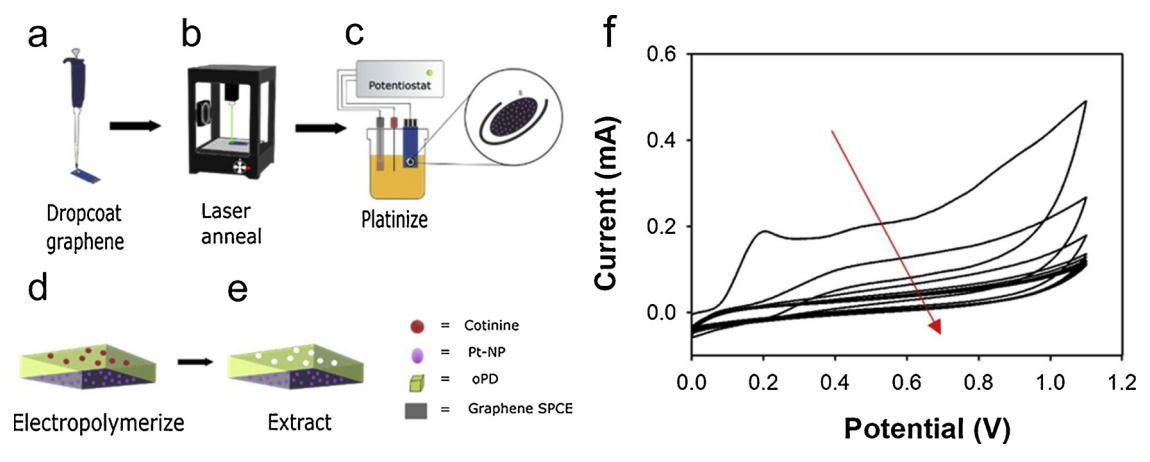
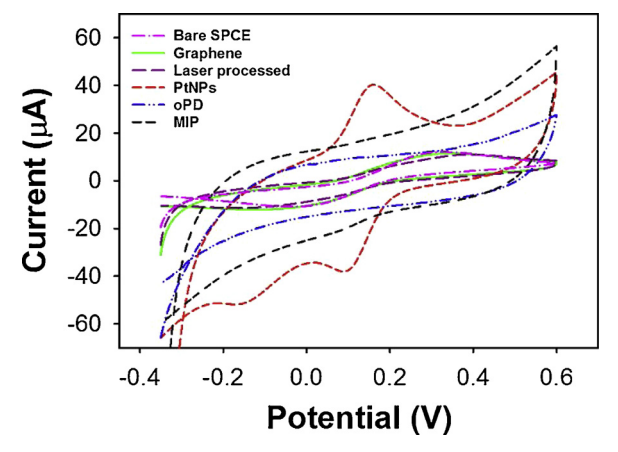


Fig. 1. Schematic of the fabrication of molecularly imprinted polymer (MIP) on a PtNP/graphene-SPCE: (a) bare PtNP/graphene-SPCE, (b) laser annealing of the drop cast graphene ink layer, (c) deposition of PtNPs, (d) electrochemical deposition of the MIP (consisting of oPD as functional monomer and cotinine as template), and (e) extraction of cotinine from the MIP. (f) Cyclic voltammogram showing electropolymerization of oPD in the presence of cotinine (MIP) for 20 cycles on the PtNP/graphene-SPCE. The red arrow points in the direction of reducing CV scan intensity for every consequent MIP electropolymerization cycle. (For interpretation of the references to colour in this figure legend, the reader is referred to the web version of this article).

Fig. 2. SEM images (15000×) of (a) bare SPCE, (b) after graphene functionalization and laser annealing & (c) electrode deposited with platinum nanoparticles.



**Fig. 3.** Cyclic voltammograms of a bare SPCE (pink) as well as SPCEs enhanced with the following cumulative modifications: graphene (green); laser processing (purple); PtNPs (red); oPD (blue); and finally, with the MIP where the cotinine is extracted from deposited oPD (black). (For interpretation of the references to colour in this figure legend, the reader is referred to the web version of this article).

(Fig. 2b), the surface turned relatively smooth, filling up deeper cavities on the graphene-SPCE. The presence of deposited PtNPs are densely packed and increase the electroactive surface area of the electrode (Fig. 2c). This increased electroactive surface area leads to higher sensor sensitivity as previously illustrated [53–55] and as illustrated in Fig. 3.

Cyclic voltammetry was next used to characterize the electroactivity of the electrode before and after various stages of nanostructuring and functionalization (Fig. 3) (see Experimental Methods). It should be noted that the oxidation current of the bare electrode does not change significantly after the functionalization with drop coated graphene and laser annealing. This negligible change in oxidation current is most likely due to the fact that multiple layers of relatively 'smooth' graphene present on the electrode electrochemically behave much like bulk carbon, that is, these multiple layers of graphene are similar in electroreactivity to the bare SPCE surface. However, the electrodeposition of PtNPs on the electrode increases the current by almost 4fold from  $10\,\mu A$  to  $40\,\mu A$ —the deposited PtNPs significantly increase the electroreactive nature of the electrode. The electrochemical deposition of PtNPs was much more efficient on graphene coated SPCEs than unmodified SPCEs and hence the drop coated graphene was deemed a necessary component of the electrode fabrication. This increase in ability to deposit Pt nanoparticles is most likely due to the increased graphene defect sites that the laser creates on the deposited graphene flakes [40,41]. Also, further rationale for the inclusion of graphene and PtNPs into the electrode design is detailed in subsequent sections where the graphene-PtNP modified SPCEs enabled electrochemical monitoring of cotinine after biofunctionalization with the MIP while the bare SPCE functionalized with the MIP did not have sufficient

sensitivity for cotinine sensing. Finally, the electropolymerization of the oPD electrode leads to diminished oxidation current which is expected as this polymer is electrically non-conducting.

The extraction of cotinine from MIP created pores that are of the same shape and size of cotinine molecules (see Experimental Methods). These pores help in enabling the interaction of the ferro/ferricyanide probe with the PtNP/graphene-SPCE surface, leading to higher current with respect to deposited MIP. This current peak is not as high as the one associated with the electrode subsequently platinized with PtNPs because the entire surface of the electrode is not accessible to the ferro/ferricyanide redox probe; only the fraction of the electrode surface area exposed after MIP extraction is accessible to the redox probe. These CV characteristics show similar behavior to previously reported MIP based sensors where the electrode surface has been modified with metallic nanoparticles for improving the sensitivity / electroactivity of electrodes and consequently the sensitivity of the resultant electrochemical biosensor [58].

## 3.3. Electrochemical cotinine sensing characterization

The developed MIP and NIP were next electrochemically calibrated for cotinine sensing using a 3-electrode set-up (see Experimental Methods). Briefly cotinine biosensing was conducted with the developed electrodes by incubating distinct concentrations of cotinine  $(0.1 \text{ nM}, 1 \text{ nM}, 5 \text{ nM}, 10 \text{ nM}, 50 \text{ nM}, 100 \text{ nM}, 1 \text{ } \mu\text{M}, 10 \text{ } \mu\text{M})$  in phosphate buffer solution first for 10 min and then cycling the voltage during CV over the potential range of -0.35 V and 0.6 V (Fig. S2). The change in the peak oxidation of the distinct CVs was used for the cotinine calibration plot (Fig. 4a). A linear relationship between the oxidation current and cotinine concentration was observed across a wide linear range of 1-100 nM (current change of 9 µA) for the PtNP/graphene-SPCE functionalized with the MIP while the bare SPCE modified with the MIP displayed negligible change in the normalized oxidation current with increasing concentration of cotinine. Moreover, the correlation coefficient (R<sup>2</sup>) for the linear sensing range was obtained to be 0.95 and the detection limit (calculated by considering thrice the standard deviation of the background signal obtained from the y-intercept of the cotinine linear regression calibration plot (i.e.,  $3\sigma$ ) or in other words considering the regression equation as y = mx + b, substitute 30 from the background noise for y and determine 'x' as the concentration for detection limit [31]) was found to be 0.97 nM for the PtNP/graphene-SPCE functionalized with the MIP (Fig. 4b). In the Fig. 4b, the x-axis has been converted to the logarithmic value of the concentration for convenience of representation and calculation. Oxidation peak current increases with higher values of cotinine concentration (Fig. 4a) and consequently indicates rising electron transfer from cotinine molecules solvated in aqueous phosphate buffer solution owing to its alkaline nature (electron pair on the nitrogen atoms) in the buffer medium [61] to the electrode. It is important to note here that this increase in current response is opposite to a decrease in current response which would be expected for typical non-electroactive

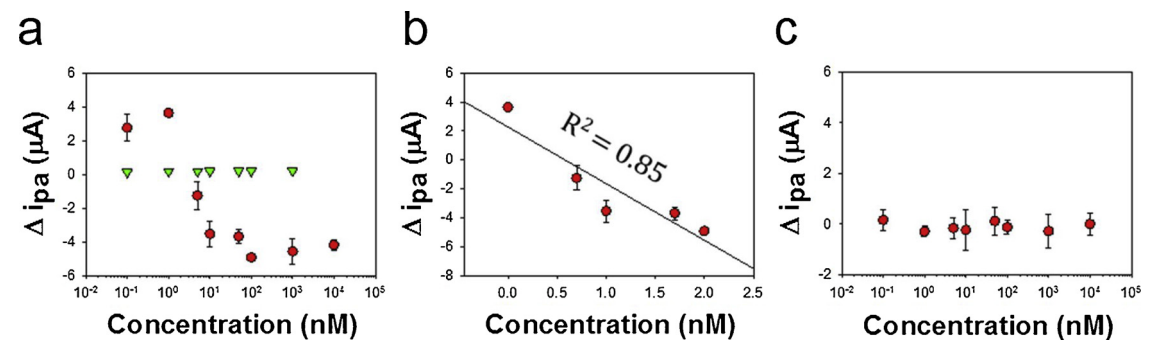


Fig. 4. (a) Relationship between change of peak current and incubation with increasing concentrations of cotinine in PBS buffer: PtNP/graphene-SPCE functionalized with the MIP (red) and a bare SPCE functionalized with the MIP (green). The error bars are not visible for bare SPCE data points because the error is in the range of 0.030-0.0421  $\mu$ A. (b) Regression line (equation: y = -3.9218x + 2.2809) fitted to the calibration curve for cotinine sensing in PBS (x-axis values have been converted to log values). (c) Control experiment demonstrating the variation of the oxidation peak current for different concentration of cotinine with non-imprinted polymer (NIP). The error bars on the data points indicate standard deviation of experiments for n = 2. (For interpretation of the references to colour in this figure legend, the reader is referred to the web version of this article).

analytes that selectively bind to the MIP cavities and prevent the diffusion of the electrochemical probe (i.e. ferricyanide) into the imprinted cavities and consequently decrease current response with increasing concentration [28]. Hence, in this developed MIP biosensor, the increase in electron transfer from the MIP bound cotinine molecules to the underlying graphene electrode is greater than the decrease in signal response expected from the diffusional impediment of the ferricyanide redox probe to the electrode surface. The control NIP exhibited negligible oxidation current changes with increasing concentration of cotinine solution (Fig. 4c).

# 3.4. Electrochemical cotinine selectivity experiments and testing in saliva samples

Selectivity of the MIP towards cotinine was evaluated by testing the sensitivity of the sensor to nicotine and myosmine. Nicotine and myosmine are alkaloids like cotinine that are similar in molecular structure and weight to cotinine [17]. Since the working mechanism of MIP relies on the molecular structure of the pores left behind by the target species, determining the selectivity of such MIP-based biosensors is a crucial step to validate the potential efficacy of the sensor in actual saliva samples. Here, the MIP was exposed to various amounts of these interfering species (10, 50, and 100 nM respectively). These concentrations are well beyond the nicotine and cotinine saliva concentration values ( $\sim 61.6\,\mathrm{nM}$  and 56.7 nM respectively) that have been noted to determine active smoking versus passive exposure [62] or in the case of myosmine are concentrations much higher than would be found in a smoker or nonsmoker ( $\sim 17.4\,\mathrm{and}\,5.0\,\mathrm{nM}$  respectively) [63].

Both interfering species display negligible current response change

during experiments with the ferro/ferricyanide probe (Fig. 5a). These observations illustrate the presence of cavities within the MIP that are highly specific to cotinine binding. It should be noted here that cotinine conforms to these cavities *via* weak hydrogen bonds and Van der Waals interactions. However, the lack of carbonyl groups in nicotine and lack of both carbonyl and methyl groups in myosmine most likely prohibits the adsorption of these species into the MIP cavities as they prevent formation of hydrogen bonds or Van der Waals interaction within the cavity [5,33,64].

The MIP sensor was next characterized with human saliva samples. The MIP biosensor was incubated with the saliva supernatant and cotinine calibration plots via ferrocyanide CV were performed by spiking the solution with cotinine concentrations of 1 nM, 5 nM, 10 nM, 50 nM and 1  $\mu$ M (see Experimental Methods). These calibration plots revealed that the oxidation peak current of the probe decreases linearly with concentration of cotinine in the range of 1-100 nM (Fig. 5b). The correlation coefficient was calculated to be 0.99 with a low cotinine detection limit of 0.33 nM (Fig. 5c) (In the Fig. 5c, the x-axis has been converted to the logarithmic value of the concentration for convenience of representation and calculation of detection limit using the regression equation). Hence the developed biosensor is able to detect cotinine saliva concentration levels that are an order of magnitude lower than those reported in saliva in smokers (40-74 nM) [15]. It should also be noted here that the oxidation peak current values of the CV plots decrease with higher cotinine concentration (see Fig. S3 in Supplemental Information). Moreover, these cotinine protein/DNA complexes also physically block the existing cavities in MIP and prevent the ferro/ ferricyanide probe from reacting with the electrode surface [59]. Hence electron transfer between the ferrocyanide redox probe and the

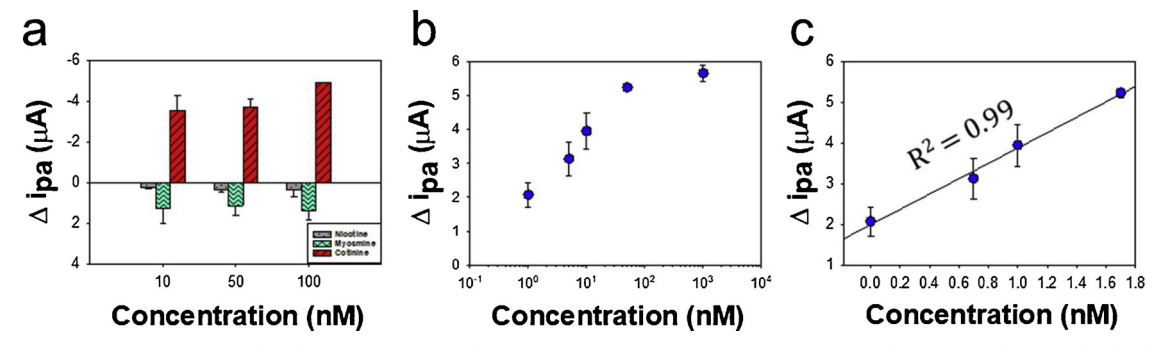


**Fig. 5.** (a) Interference test of cotinine (red) with nicotine (grey) and myosmine (cyan) at concentration of 10, 50 and 100 nM each in PBS buffer, the error bar on cotinine for 100 nM is not visible as the error is 0.007; (b) Relationship between change of peak current and incubation with increasing concentrations of cotinine in real saliva sample; (c) Regression line (equation: y = 1.8891x + 1.9965) fitted to the calibration curve for cotinine sensing in saliva (x-axis values have been converted to log values). (For interpretation of the references to colour in this figure legend, the reader is referred to the web version of this article).

 Table 1

 Performance comparison table of cotinine biosensors.

Detection technique	Linear sensing range	Detection limit	Media	Reference
Molecularly imprinted solid-phase extraction	170.1 nM - 2.835 u M	56.7 nM	Saliva	[5]
SERS with thin-layer chromatography	40 nM - 8 uM	10 nM	Urine	[10]
MIP: electrical conductivity, gas chromatography, infrared spectroscopy	_	283.5 nM	Toluene solution	[16]
Piezoelectric microgravimetry MIP	1-10 mM	1.2 mM	-	[17]
MIP solid phase extraction and liquid-liquid extraction	56.7 nM - 22.68 uM	17.01 nM	Urine	[21]
Immunochromatography	5.67 - 567 nM	5.67 nM	Serum	[23]
Chemiluminescence immunoassay	56.7 nM – 5.67 uM	28.35 nM	Mouse serum	[31]
MIP using electrochemical detection	1-100 nM	0.33 nM	Saliva	This work

Legend: MIP - Molecularly Imprinted Polymer; SERS - Surface Enhanced Raman Spectroscopy.

electrode is diminished as higher concentrations of cotinine are introduced to the saliva supernatant.

The overall sensing results of the PtNP/graphene-SPCE functionalized with the MIP is advantageous for a variety of reasons (Table 1). This biosensor offers a wide sensing range and lower detection limit than other cotinine sensors, and spans the range of cotinine concentrations found in even light smokers and passive smokers [15]. The total time to obtain a reading from the developed biosensor is approximately 11-12 min, including the incubation time of cotinine (  $\sim\!10$  min.) and acquisition of CVs (  $\sim\,1\text{--}2\,\text{min})$  which is a much shorter sensing time than laboratory techniques such as gas chromatography and impedance measurement techniques that require 20-68 minutes to obtain a measurement [16,30]. Finally, this MIP biosensor exhibits a lower detection limit than published cotinine sensors (see Table 1). Moreover, the developed biosensors are amenable for use with human saliva. Such human saliva can be non-invasively collected from patients to rapidly sense cotinine levels without the need for adulteration (no need for mixture with an artificial medium such as toluene) to assess smoking exposure / tobacco use. Studies have also shown that saliva cotinine levels reach higher concentrations compared to other biological media like urine or blood and hence saliva is a bodily fluid wellsuited for cotinine sensing [65]. Therefore, the developed biosensor is amenable to in-field cotinine monitoring where non-invasive bodily fluid acquisition and minimal sample processing is critically important for wide scale implementation.

# 4. Conclusion

A cotinine-based MIP biosensor was created by coating a SPCE with laser annealed graphene, electrochemically deposited PtNPs and finally an oPD-based MIP. The resultant MIP biosensor displayed a high sensitivity to cotinine (1.89 µA/decade) over a wide linear sensing range (1–100 nM) and with a low detection limit (0.33 nM) in saliva samples. Such nanostructuring of the SPCE was necessary to obtain measurable cotinine readings with this MIP functionalization approach. The selectivity of the biosensor was further tested with similar molecular alkaloids (i.e., nicotine and myosmine). These chemical analogs were tested and displayed negligible biosensor signal response even at elevated concentrations that are relevant for determining tobacco use in patients. Moreover, each cotinine measurement can be obtained within 11-12 minutes. Hence the sensitivity, selectivity, and rapid nature of the developed MIP biosensor make it is well-suited for biosensing at various point-of-service applications such as when a person's smoking status must be divulged as needed in employment interviews or for the proper establishment of health insurance premiums. Due to the high sensitivity of the biosensor, the developed MIP biosensor could also be used to help distinguish between smoke ingestion from actual smokers or from secondhand smoke. Such information could be useful to pass legislation that ensures high smoke-free air quality in public places like hospitals, office buildings or schools as well as to pass guidelines for smoking in private locations. In even broader terms this protocol for

synthesizing MIP by electropolymerization of oPD could be applied for a wide variety of other target species such as neurotransmitters [66,67], proteins [22] and chemical compounds [33,59]. The fabrication method developed herein is also a one-step, batch process for producing MIP in a rapid fashion as the electrochemical deposition process is performed in a bath of monomer and template solution, as opposed to other techniques that require longer polymerization steps such as thermal polymerization and sedimentation [5,19]. Hence, the developed MIP biosensor could act as a low-cost, point-of-service biosensor that could be modified for a wide variety of diagnostic and analyte monitoring applications including for the use of protein transport [68], bacteria detection [69,70], food and agriculture applications [71,72], and various diagnostic assays [73].

## Acknowledgements

The authors gratefully acknowledge funding support from the National Institute of Food and Agriculture, U.S. Department of Agriculture, under Award Number 2016-67021-25038, the National Science Foundation under award number CBET1706994, as well as by the Iowa State University College of Engineering and Department of Mechanical Engineering.

# Appendix A. Supplementary data

Supplementary material related to this article can be found, in the online version, at doi:https://doi.org/10.1016/j.snb.2019.02.032.

## References

- W.J. Blot, J.K. McLaughlin, D.M. Winn, D.F. Austin, R.S. Greenberg, S. Preston-Martin, et al., Smoking and drinking in relation to oral and pharyngeal cancer, Cancer Res. 48 (1988) 3282–3287.
- [2] K. Jayant, V. Balakrishnan, L. Sanghvi, D. Jussawalla, Quantification of the role of smoking and chewing tobacco in oral, pharyngeal, and oesophageal cancers, Br. J. Cancer 35 (1977) 232.
- [3] P. Jha, Avoidable global cancer deaths and total deaths from smoking, Nat. Rev. Cancer 9 (2009) 655.
- [4] R. Khlifi, A. Hamza-Chaffai, Head and neck cancer due to heavy metal exposure via tobacco smoking and professional exposure: a review, Toxicol. Appl. Pharmacol. 248 (2010) 71–88.
- [5] R.V. Vitor, M.C. Martins, E.C. Figueiredo, I. Martins, Application of molecularly imprinted polymer solid-phase extraction for salivary cotinine, Anal. Bioanal. Chem. 400 (2011) 2109–2117.
- [6] J.T. Hays, I.T. Croghan, D.R. Schroeder, K.P. Offord, R.D. Hurt, T.D. Wolter, et al., Over-the-counter nicotine patch therapy for smoking cessation: results from randomized, double-blind, placebo-controlled, and open label trials, Am. J. Public Health 89 (1999) 1701–1707.
- [7] M.M. Schuurmans, A.H. Diacon, X. Van Biljon, C.T. Bolliger, Effect of pre-treatment with nicotine patch on withdrawal symptoms and abstinence rates in smokers subsequently quitting with the nicotine patch: a randomized controlled trial, Addiction 99 (2004) 634–640.
- [8] D.A. Kidwell, J.C. Holland, S. Athanaselis, Testing for drugs of abuse in saliva and sweat, J. Chromatogr. B Biomed. Sci. Appl. 713 (1998) 111–135.
- [9] D.W. Sepkovic, N.J. Haley, Biomedical applications of cotinine quantitation in smoking related research, Am. J. Public Health 75 (1985) 663–665.
- [10] R. Huang, S. Han, X.S. Li, Detection of tobacco-related biomarkers in urine samples by surface-enhanced Raman spectroscopy coupled with thin-layer chromatography,

<sup>\*</sup>Note: concentration values have been converted to Molar concentrations to improve comparison.

- Anal. Bioanal. Chem. 405 (2013) 6815-6822.
- [11] J. Kemmeren, G. Vanpoppel, P. Verhoef, M. Jarvis, Plasma cotinine: stability in smokers and validation of self-reported smoke exposure in nonsmokers, Environ. Res. 66 (1994) 235–243.
- [12] H. Kim, Y. Lim, S. Lee, S. Park, C. Kim, C. Hong, et al., Relationship between environmental tobacco smoke and urinary cotinine levels in passive smokers at their residence, J. Expo. Anal. Environ. Epidemiol. 14 (Suppl 1) (2004) S65–70.
- [13] N.L. Benowitz, Cotinine as a biomarker of environmental tobacco smoke exposure, Epidemiol. Rev. 18 (1996) 188–204.
- [14] N.L. Benowitz, J.T. Bernert, R.S. Caraballo, D.B. Holiday, J. Wang, Optimal serum cotinine levels for distinguishing eigarette smokers and nonsmokers within different racial/ethnic groups in the United States between 1999 and 2004, Am. J. Epidemiol. 169 (2009) 236–248.
- [15] J.-F. Etter, T.V. Due, T.V. Perneger, Saliva cotinine levels in smokers and non-smokers, Am. J. Epidemiol. 151 (2000) 251–258.
- [16] S. Antwi-Boampong, K.S. Mani, J. Carlan, J.J. BelBruno, A selective molecularly imprinted polymer-carbon nanotube sensor for cotinine sensing, J. Mol. Recognit. 27 (2014) 57–63.
- [17] K. Noworyta, W. Kutner, C.A. Wijesinghe, S.G. Srour, F. D'Souza, Nicotine, cotinine, and myosmine determination using polymer films of tailor-designed zinc porphyrins as recognition units for piezoelectric microgravimetry chemosensors, Anal. Chem. 84 (2012) 2154–2163.
- [18] D.C. Apodaca, R.B. Pernites, R.R. Ponnapati, F.R. Del Mundo, R.C. Advincula, Electropolymerized molecularly imprinted polymer films of a bis-terthiophene dendron: folic acid quartz crystal microbalance sensing, ACS Appl. Mater. Interfaces 3 (2011) 191–203.
- [19] J. Alenus, A. Ethirajan, F. Horemans, A. Weustenraed, P. Csipai, J. Gruber, et al., Molecularly imprinted polymers as synthetic receptors for the QCM-D-based detection of L-nicotine in diluted saliva and urine samples, Anal. Bioanal. Chem. 405 (2013) 6479–6487.
- [20] C. Malitesta, E. Mazzotta, R.A. Picca, A. Poma, I. Chianella, S.A. Piletsky, MIP sensors-the electrochemical approach, Anal. Bioanal. Chem. 402 (2012) 1827–1846.
- [21] M.C.G. Martins, P.P. Maia, V. Bergamin Boralli, E.C. Figueiredo, I. Martins, Determination of cotinine in urine by molecularly imprinted polymer solid phase and liquid–Liquid extraction coupled with gas chromatography, Anal. Lett. 48 (2015) 1245–1256.
- [22] V.V. Shumyantseva, T.V. Bulko, L.V. Sigolaeva, A.V. Kuzikov, A.I. Archakov, Electrosynthesis and binding properties of molecularly imprinted poly-o-phenylenediamine for selective recognition and direct electrochemical detection of myoglobin, Biosens, Bioelectron, 86 (2016) 330–336.
- [23] H. Nian, J. Wang, H. Wu, J.G. Lo, K.H. Chiu, J.G. Pounds, et al., Electrochemical immunoassay of cotinine in serum based on nanoparticle probe and immunochromatographic strip, Anal. Chim. Acta 713 (2012) 50–55.
- [24] G.F. Cope, H.H. Wu, G.V. O'Donovan, H.J. Milburn, A new point of care cotinine test for saliva to identify and monitor smoking habit, Eur. Respir. J. 40 (2012) 496–497.
- [25] G.F. Marrone, M. Paulpillai, R.J. Evans, E.G. Singleton, S.J. Heishman, Breath carbon monoxide and semiquantitative saliva cotinine as biomarkers for smoking, Hum. Psychopharmacol. Clin. Exp. 25 (2010) 80–83.
- [26] N.J. Montalto, W.O. Wells, Validation of self-reported smoking status using saliva cotinine: a rapid semiquantitative dipstick method, Cancer Epidemiol. Prevent. Biomark 16 (2007) 1858–1862.
- [27] A. Zgierska, M.L. Wallace, C.A. Burzinski, J. Cox, M. Backonja, Pharmacological and toxicological profile of opioid-treated, chronic low back pain patients entering a mindfulness intervention randomized controlled trial, J. Opioid Manag. 10 (2014) 323
- [28] C. Malitesta, E. Mazzotta, R.A. Picca, A. Poma, I. Chianella, S.A. Piletsky, MIP sensors – the electrochemical approach, Anal. Bioanal. Chem. 402 (2012) 1897–1846
- [29] G. Vasapollo, R.D. Sole, L. Mergola, M.R. Lazzoi, A. Scardino, S. Scorrano, et al., Molecularly imprinted polymers: present and future prospective, Int. J. Mol. Sci. 12 (2011) 5908–5945.
- [30] R. Thoelen, R. Vansweevelt, J. Duchateau, F. Horemans, J. D'Haen, L. Lutsen, et al., A MIP-based impedimetric sensor for the detection of low-MW molecules, Biosens. Bioelectron. 23 (2008) 913–918.
- [31] W. Liu, C.L. Cassano, X. Xu, Z.H. Fan, Laminated paper-based analytical devices (LPAD) with origami-enabled chemiluminescence immunoassay for cotinine detection in mouse serum, Anal. Chem. 85 (2013) 10270–10276.
- [32] M.S. Abdelkader, B. Lockwood, P. Sansongsak, Uptake of nicotine from suspension culture of Nicotiana tabacum by molecularly imprinted polymers, J. Pharm. Pharmacol. 62 (2010) 633–637.
- [33] Y. Hu, S. Feng, F. Gao, E.C. Li-Chan, E. Grant, X. Lu, Detection of melamine in milk using molecularly imprinted polymers-surface enhanced Raman spectroscopy, Food Chem. 176 (2015) 123–129.
- [34] R. Kecili, J. Billing, D. Nivhede, B. Sellergren, A. Rees, E. Yilmaz, Fast identification of selective resins for removal of genotoxic aminopyridine impurities via screening of molecularly imprinted polymer libraries, J. Chromatogr. A 1339 (2014) 65–72.
- [35] A.L.M. Ruela, E.C. Figueiredo, G.R. Pereira, Molecularly imprinted polymers as nicotine transdermal delivery systems, Chem. Eng. J. 248 (2014) 1–8.
- [36] H. Sambe, K. Hoshina, R. Moaddel, I.W. Wainer, J. Haginaka, Uniformly-sized, molecularly imprinted polymers for nicotine by precipitation polymerization, J. Chromatogr. A 1134 (2006) 88–94.
- [37] T. Sergeyeva, S. Piletsky, A. Brovko, E. Slinchenko, L. Sergeeva, A. El'Skaya, Selective recognition of atrazine by molecularly imprinted polymer membranes. Development of conductometric sensor for herbicides detection, Anal. Chim. Acta

- 392 (1999) 105-111.
- [38] H.-J. Wang, W.-H. Zhou, X.-F. Yin, Z.-X. Zhuang, H.-H. Yang, X.-R. Wang, Template synthesized molecularly imprinted polymer nanotube membranes for chemical separations, J. Am. Chem. Soc. 128 (2006) 15954–15955.
- [39] N. Karimian, M. Vagin, M.H. Zavar, M. Chamsaz, A.P. Turner, A. Tiwari, An ultrasensitive molecularly-imprinted human cardiac troponin sensor, Biosens. Bioelectron. 50 (2013) 492–498.
- [40] J.A. Hondred, L.R. Stromberg, C.L. Mosher, J.C. Claussen, High-Resolution Graphene Films for Electrochemical Sensing via Inkjet Maskless Lithography, ACS Nano 11 (2017) 9836–9845.
- [41] S.R. Das, Q. Nian, A.A. Cargill, J.A. Hondred, S. Ding, M. Saei, et al., 3D nanos-tructured inkjet printed graphene via UV-pulsed laser irradiation enables paper-based electronics and electrochemical devices, Nanoscale 8 (2016) 15870–15879.
- [42] S.R. Das, S. Srinivasan, L.R. Stromberg, Q. He, N. Garland, W.E. Straszheim, et al., Superhydrophobic inkjet printed flexible graphene circuits via direct-pulsed laser writing, Nanoscale 9 (2017) 19058–19065.
- [43] V. Di Noto, E. Negro, R. Gliubizzi, S. Lavina, G. Pace, S. Gross, et al., A Pt–Fe carbon nitride nano-electrocatalyst for polymer electrolyte membrane fuel cells and direct-methanol fuel cells: synthesis, characterization, and electrochemical studies, Adv. Funct. Mater. 17 (2007) 3626–3638.
- [44] Y. Zhao, L. Fan, H. Zhong, Y. Li, S. Yang, Platinum nanoparticle clusters immobilized on multiwalled carbon nanotubes: electrodeposition and enhanced electrocatalytic activity for methanol oxidation, Adv. Funct. Mater. 17 (2007) 1537–1541.
- [45] J.C. Claussen, M.A. Daniele, J. Geder, M. Pruessner, A.J. Makinen, B.J. Melde, et al., Platinum-paper micromotors: an urchin-like nanohybrid catalyst for green monopropellant bubble-thrusters, ACS Appl. Mater. Interfaces 6 (2014) 17837–17847.
- [46] K.M. Marr, B. Chen, E.J. Mootz, J. Geder, M. Pruessner, B.J. Melde, et al., High aspect ratio carbon nanotube membranes decorated with Pt nanoparticle urchins for micro underwater vehicle propulsion via H2O2 decomposition, ACS Nano 9 (2015) 7791–7803.
- [47] B. Chen, N.T. Garland, J. Geder, M. Pruessner, E. Mootz, A. Cargill, et al., Platinum nanoparticle decorated SiO2 microfibers as catalysts for Micro unmanned underwater vehicle propulsion, ACS Appl. Mater. Interfaces 8 (2016) 30941–30947.
- [48] J.C. Claussen, A. Kumar, D.B. Jaroch, M.H. Khawaja, A.B. Hibbard, D.M. Porterfield, et al., Nanostructuring platinum nanoparticles on multilayered graphene petal nanosheets for electrochemical biosensing, Adv. Funct. Mater. 22 (2012) 3399–3405.
- [49] S. Hrapovic, E. Majid, Y. Liu, K. Male, J.H. Luong, Metallic nanoparticle carbon nanotube composites for electrochemical determination of explosive nitroaromatic compounds, Anal. Chem. 78 (2006) 5504–5512.
- [50] J. Wang, Nanomaterial-based electrochemical biosensors, Analyst 130 (2005) 421–426.
- [51] Q. He, S.R. Das, N.T. Garland, D. Jing, J.A. Hondred, A.A. Cargill, et al., Enabling inkjet printed graphene for ion selective electrodes with postprint thermal annealing. ACS Appl. Mater. Interfaces 9 (2017) 12719–12727.
- [52] J.A. Hondred, J.C. Breger, N.J. Alves, S.A. Trammell, S.A. Walper, I.L. Medintz, et al., Printed graphene electrochemical biosensors fabricated by inkjet maskless lithography for rapid and sensitive detection of organophosphates, ACS Appl. Mater. Interfaces 10 (2018) 11125–11134.
- [53] W. Lian, S. Liu, J. Yu, X. Xing, J. Li, M. Cui, et al., Electrochemical sensor based on gold nanoparticles fabricated molecularly imprinted polymer film at chitosan-platinum nanoparticles/graphene-gold nanoparticles double nanocomposites modified electrode for detection of erythromycin, Biosens. Bioelectron. 38 (2012) 163–169.
- [54] P.T. Yin, T.H. Kim, J.W. Choi, K.B. Lee, Prospects for graphene-nanoparticle-based hybrid sensors, Phys. Chem. Chem. Phys. 15 (2013) 12785–12799.
- [55] M. Zhang, C. Liao, C.H. Mak, P. You, C.L. Mak, F. Yan, Highly sensitive glucose sensors based on enzyme-modified whole-graphene solution-gated transistors, Sci. Rep. 5 (2015) 8311.
- [56] G. Camurri, P. Ferrarini, R. Giovanardi, R. Benassi, C. Fontanesi, Modelling of the initial stages of the electropolymerization mechanism of o-phenylenediamine, J. Electroanal. Chem. 585 (2005) 181–190.
- [57] J. Li, F. Jiang, X. Wei, Molecularly imprinted sensor based on an enzyme amplifier for ultratrace oxytetracycline determination, Anal. Chem. 82 (2010) 6074–6078.
- [58] T. Li, T. Yao, C. Zhang, G. Liu, Y. She, M. Jin, et al., Electrochemical detection of ractopamine based on a molecularly imprinted poly-o-phenylenediamine/gold nanoparticle-ionic liquid-graphene film modified glass carbon electrode, RSC Adv. 6 (2016) 66949–66956.
- [59] X. Li, Y. He, F. Zhao, W. Zhang, Z. Ye, Molecularly imprinted polymer-based sensors for atrazine detection by electropolymerization of o-phenylenediamine, RSC Adv. 5 (2015) 56534–56540.
- [60] L. Chimuka, M. van Pinxteren, J. Billing, E. Yilmaz, J.Å. Jönsson, Selective extraction of triazine herbicides based on a combination of membrane assisted solvent extraction and molecularly imprinted solid phase extraction, J. Chromatogr. A 1218 (2011) 647–653.
- [61] A. Pezzolato, Abstracts of papers on organic chemistry, in: F.R.S.C.E. Groves (Ed.), J Chem Soc, Chemical Society, London, 1893, p. 444 N. (R.).
- [62] S. Feng, O. Cummings, G. McIntire, Nicotine and cotinine in oral fluid: passive exposure vs active smoking, Pract. Lab. Med. 12 (2018) e00104.
- [63] K. Schütte-Borkovec, C.W. Heppel, A.-K. Heling, E. Richter, Analysis of myosmine, cotinine and nicotine in human toenail, plasma and saliva, Biomarkers 14 (2009) 278–284.
- [64] F.L. Dickert, O. Hayden, Molecular fingerprints using imprinting techniques, Adv. Mater. 12 (2000) 311–314.
- [65] Y. Shafagoj, F. Mohammed, K. Hadidi, Hubble-bubble (water pipe) smoking: levels of nicotine and cotinine in plasma, saliva and urine, Int. J. Clin. Pharmacol. Ther.

- 40 (2002) 249-255.
- [66] X. Liu, H. Zhu, X. Yang, An electrochemical sensor for dopamine based on poly(ophenylenediamine) functionalized with electrochemically reduced graphene oxide, RSC Adv. 4 (2014) 3743–3749.
- [67] D. Wu, H. Li, X. Xue, H. Fan, Q. Xin, Q. Wei, Sensitive and selective determination of dopamine by electrochemical sensor based on molecularly imprinted electropolymerization of o-phenylenediamine, Anal. Methods 5 (2013).
- [68] J. Orozco, A. Cortés, G. Cheng, S. Sattayasamitsathit, W. Gao, X. Feng, et al., Molecularly imprinted polymer-based catalytic micromotors for selective protein transport, J. Am. Chem. Soc. 135 (2013) 5336–5339.
- [69] L. Uzun, A.P. Turner, Molecularly-imprinted polymer sensors: realising their

- potential, Biosens. Bioelectron. 76 (2016) 131-144.
- [70] M. Zourob, S. Elwary, A.P. Turner, Principles of Bacterial Detection: Biosensors, Recognition Receptors and Microsystems, Springer Science & Business Media, 2008.
- [71] S. Gunasekaran, 8 nanotechnology for food: principles and selected applications, Food Processing: Principles and Applications, (2014), pp. 171–205.
- [72] L.M. Kindschy, E.C. Alocilja, A review of molecularly imprinted polymers for biosensor development for food and agricultural applications, Trans. ASAE 47 (2004) 1375.
- [73] T.S. Bedwell, M.J. Whitcombe, Analytical applications of MIPs in diagnostic assays: future perspectives, Anal. Bioanal. Chem. 408 (2016) 1735–1751.